Available online at www.sciencedirect.com
ScienceDirect
Journal of Computational and Applied Mathematics 222 (2008) 487–499
JOURNAL OF COMPUTATIONAL AND APPLIED MATHEMATICS
www.elsevier.com/locate/cam

Shape-topology optimization for Navier–Stokes problem using variational level set method☆

Xian-Bao Duan[a,*], Yi-Chen Ma[a], Rui Zhang[b]

[a] *School of Science, Xi'an Jiaotong University, Xi'an 710049, PR China*
[b] *Institute of Applied Mathematics, Shandong University of Technology, Zibo 255049, PR China*

Received 18 June 2007; received in revised form 14 November 2007

Abstract

We consider the shape-topology optimization of the Navier–Stokes problem. A new algorithm is proposed based on the variational level set method. By this algorithm, a relatively smooth evolution can be maintained without re-initialization and drastic topology change can be handled easily. Finally, the promising features of the proposed method are illustrated by two benchmark examples.

MSC: 49Q10; 49Q12; 35Q30; 93B40

Keywords: Navier–Stokes problem; Shape-topology optimization; Sensitivity analysis; Variational level set method

1. Introduction

Shape or topology optimization is to find the optimal shape or topology of a domain which minimizes or maximizes a given criterion (often called a cost function). The shape optimization of the fluid flow has long been a subject of interest to engineers and scientists and the applications are uncountable. The biggest demand for shape optimization is for airplanes [6,9,13,14,31,42], for which even a small drag decrease means a lot of savings [37]. This method has also been used in other related fields. For instance, Agoshkov, Quarteroni and Rozza [2,3,41] apply the optimal control approaches to shape optimization of aorto-coronaric bypass anastomoses. Unlike the case of classical shape optimization, in topology optimization the structure of the domain may change during the optimization process. A new and very interesting application of the topology optimization method is for fluid flow [11,17,25]. For more works in shape or topology optimization of fluid flow, we refer to [10,28,30,37,36] and references therein.

The classical method of shape sensitivity, which has been much studied [15,16,46,50], is a very general method that can handle any type of cost functional and fluid models. But this method was implemented in a Lagrangian framework, a remeshing process is always necessary and cannot be avoided in most cases, hence it is very time-consuming [4].

☆ This work is supported by the National Natural Science Foundation of China, Grant No. 10671153, 10371096.
* Corresponding author.
E-mail address: xbduan@mail.xjtu.edu.cn (X.-B. Duan).

0377-0427/$ - see front matter © 2007 Elsevier B.V. All rights reserved.
doi:10.1016/j.cam.2007.11.016

The idea of the fictitious domain method is to extend the equations defined in a more complex domain of interest to a much simpler domain that can be easily discretized using regular, uniform elements. All the computations are carried out on this simpler domain which facilitates the parallelization of the process. The extension of the equations is such that the extended solution, when restricted to the original domain, coincides with the solution of the original problem. Due to the regularity of the meshes, faster solvers can be adopted [30]. Glowinski and collaborators have extensively developed fictitious domain methods to solve complicated problems in regular grids [19–24]. Many works in immersed domain/boundary methods [1,33,35] share similar ideas to fictitious domain methods. In shape optimization, fictitious domain methods are even more appealing since they avoid the difficulties associated with a remeshing procedure. A comparison of some fictitious domain methods used in shape optimization can be found in [29].

The level set method, first devised by Osher and Sethian [39,40], has been recently introduced in the field of shape or topology optimization, enabling a smooth representation of the boundaries on a fixed mesh and therefore leading to a fast numerical algorithm [4,5,7,49]. The main idea of the level set method for optimization problems is to choose the direction (velocity) in such a way that a decrease of the cost functional is achieved, which assembles the classical speed method in shape optimization. Sethian and Wiegmann [44] are among the first researchers to extend the level set method to capture the free boundary of a structure on a fixed Eulerian mesh. The work of Allaire et al. [4,5] combines sensitivity analysis and level set methods to perform structural optimization in two and three dimensions. Osher and Santosa [38] investigated a two-phase optimization of a membrane modeled by a linear scalar partial differential equation. Wang et al. [49] established the speed (or velocity) vector in terms of the shape of the boundary and the variational sensitivity as a physically meaningful link between the general structural topology optimization process and the powerful level set methods. The level set methods were further developed as a natural setting to combine the rigorous shape variations into the conventional structural topology optimization process in [48]. The books [40,43] and the references cited therein provide an overview of many related works.

In conventional level set methods, the moving fronts or interfaces are represented by the zero level set. But this may not be maintained during the evolution. To solve this problem, the re-initialization procedure has been extensively used as a remedial measure to maintain the level set function as a signed distance function during the evolution [40,43]. But the re-initialization process is quite complicated, computationally costly, and has subtle side effects. Recently, a new variational formulation of level set method has been proposed by [12,32,34] and [51] which needs no re-initialization at all.

Since the level set methods are most commonly realized on a fixed Eulerian mesh, it is natural to think of borrowing ideas from fictitious domain methods to solve shape optimization problems. The Navier–Stokes equations describe flows of fluids ranging from certain gas motions to the lubrication of ball bearings. Thus, optimal shape control problems associated with the Navier–Stokes equations, if settled properly, have wide and valuable applications. In the present paper, we will concern ourselves with the optimal shape or topology control problems of the Navier–Stokes problem mainly based on the works of [12,34]. Numerical examples are given to illustrate the effectiveness of the present method in accuracy, convergence speed and insensitivity to initial designs in shape and topology optimization of 2D problems that has been extensively studied in the literature [11,25] and [17].

The rest of the paper is organized as follows: In the next section, we give the state equations that we want to optimize and shape sensitivity analysis; Section 3 is dedicated to the variational level set method; In Section 4, the optimization algorithm and two numerical examples are provided. The conclusions are given in the last section.

2. Setting of the problem and shape sensitivity analysis

We consider the two-dimensional incompressible fluid flow that is governed by the Navier–Stokes equations. Assume that Ω is an open and bounded domain in $\mathbb{R}^2$ with Lipschitz continuous boundary $\Gamma := \partial\Omega = \Gamma_c \cup \Gamma_d$. We are looking for a vector function $\boldsymbol{u} = (u_1, u_2)$ and a scalar function p, representing respectively the velocity and the pressure of the fluid, which are defined in Ω and satisfy the following steady-state Navier–Stokes equations:

$$\begin{cases} -\nu\Delta\boldsymbol{u} + (\boldsymbol{u}\cdot\nabla)\boldsymbol{u} + \nabla p = \boldsymbol{f}, & \text{in } \Omega \\ \operatorname{div}\boldsymbol{u} = 0, & \text{in } \Omega \\ \boldsymbol{u} = \boldsymbol{0}, & \text{on } \Gamma_c \\ \boldsymbol{u} = \boldsymbol{g}, & \text{on } \Gamma_d \end{cases} \tag{1}$$

where $\nu = 1/Re$ (Re is the Reynolds number) is the kinematic viscosity and $\boldsymbol{f}$ is the body force. Owing to the incompressibility of $\boldsymbol{u}$, the function $\boldsymbol{g}$ must satisfy the compatibility condition

$$\int_{\Gamma_c} \boldsymbol{g} \cdot \boldsymbol{n} = 0, \tag{2}$$

where $\boldsymbol{n}$ denotes the outward unit normal. Since Ω is varying during the optimization process, we introduce an open bounded domain $\mathcal{D}$, the so-called working domain, which contains all admissible shapes Ω.

The rigorous mathematical treatment for the Navier–Stokes problem (1) can be found in [18,47].

In general, the cost functional is of the form

$$\mathcal{J}(\Omega) = \int_{\Omega} j(\boldsymbol{u}, \nabla \boldsymbol{u}) \mathrm{d}x. \tag{3}$$

The optimal control problem is to find $\boldsymbol{u}$ such that the functional (3) is minimized subject to the Navier–Stokes equations (1).

In order to apply a gradient method to the minimization of (3), we will use the classical shape sensitivity analysis. Some classical notations and results are recalled here.

Let Ω be a regular open set of $\mathbb{R}^2$; we consider domains of the type

$$\Omega(\boldsymbol{h}) = (Id + \boldsymbol{h})(\Omega) := \{x + \boldsymbol{h}(x), \text{ such that } x \in \Omega\}. \tag{4}$$

For small vector field $\boldsymbol{h}$, the open set $\Omega(\boldsymbol{h})$ is one-to-one perturbation of the initial set Ω and $(Id + \boldsymbol{h})$ is a diffeomorphism in $\mathbb{R}^2$.

Definition 1 (*[46]*). The shape derivative of $\mathcal{J}(\Omega)$ at Ω is defined as the Fréchet derivative in $W^{1,\infty}(\mathbb{R}^2, \mathbb{R}^2)$ at 0:

$$\mathcal{J}((Id + \boldsymbol{h})(\Omega)) = \mathcal{J}(\Omega) + \mathscr{D}\mathcal{J}(\Omega)(\boldsymbol{h}) + o(\boldsymbol{h}), \tag{5}$$

where $\mathscr{D}\mathcal{J}(\Omega)$ is a continuous linear form on $W^{1,\infty}(\mathbb{R}^2, \mathbb{R}^2)$.

By the Hadamard structure theorem, it is known that the directional derivative $\mathscr{D}\mathcal{J}(\Omega)(\boldsymbol{h})$ depends only on the normal trace $\boldsymbol{h} \cdot \boldsymbol{n}$ on the boundary Γ, i.e.

Lemma 2 (*[46]*). *Let Ω be a smooth bounded open set and $j(\boldsymbol{u}, \nabla \boldsymbol{u}) \in W^{1,1}(\mathbb{R}^2)$. Then the domain shape functional (3) is differentiable at Ω and*

$$\mathscr{D}\mathcal{J}(\Omega)(\boldsymbol{h}) = \int_{\Omega} \mathrm{div}(\boldsymbol{h}(x) j(\boldsymbol{u}, \nabla \boldsymbol{u})) \mathrm{d}x = \int_{\Gamma} \boldsymbol{h}(x) \cdot \boldsymbol{n}(x) j(\boldsymbol{u}, \nabla \boldsymbol{u}) \mathrm{d}s, \tag{6}$$

for any $\boldsymbol{h} \in W^{1,\infty}(\mathbb{R}^2, \mathbb{R}^2)$.

In this work, we will examine the minimize drag/energy problem where the fluid is described by (1), i.e.

$$\begin{cases} \min\limits_{\Omega \in \mathcal{D}} \mathcal{J}_{NS}(\Omega) = \int_{\Omega} |\nabla \boldsymbol{u}|^2 \mathrm{d}\Omega, \\ \text{subject to (1)}, \end{cases} \tag{7}$$

where $\mathcal{D}$ is the working domain, in which all admissible shapes Ω are included, and $\boldsymbol{u}$ is the solution of (1). An example of $\mathcal{D}$ is:

$$\mathcal{D} = \{\Omega : \Omega \subset \mathcal{D}, |\Omega| = \gamma |\mathcal{D}|\}, \tag{8}$$

where $|\bullet|$ is the area and γ is the prescribed area fraction, a constant between 0 and 1. The existence of the optimal control problem (7) can be found in [26,27].

Using Green's formula together with Lemma 2, we can deduce that

Theorem 3 (*[36]*). *Let Ω be a smooth bounded open set and $\boldsymbol{h} \in W^{1,\infty}(\mathbb{R}^2, \mathbb{R}^2)$. Assume that the data $\boldsymbol{f}$ and the solution $\boldsymbol{u}$ of (1) are smooth enough, say $\boldsymbol{f} \in \boldsymbol{H}^1(\Omega)$, $\boldsymbol{u} \in \boldsymbol{H}^2(\Omega)$. The shape derivative of $\mathcal{J}_{NS}(\Omega)$ is*

$$\mathscr{D}\mathcal{J}_{NS}(\Omega)\boldsymbol{h} = \nu \int_{\Gamma} \left[\left(\frac{\partial \boldsymbol{u}}{\partial \boldsymbol{n}} \right)^2 - \frac{\partial \boldsymbol{u}}{\partial \boldsymbol{n}} \frac{\partial \boldsymbol{w}}{\partial \boldsymbol{n}} \right] (\boldsymbol{h}, \boldsymbol{n}) \mathrm{d}s, \tag{9}$$

where $(\boldsymbol{u}, p)$ is the solution of the problem (1) and $(\boldsymbol{w}, q)$ is the solution of the following adjoint equations

$$\begin{cases} -\nu \Delta \boldsymbol{w} - ((\boldsymbol{u} \cdot \nabla)\boldsymbol{w} + (\nabla \boldsymbol{w})\boldsymbol{u}) + \nabla q = -2\nu \Delta \boldsymbol{u}, & in\ \Omega \\ \nabla \cdot \boldsymbol{w} = 0, & in\ \Omega \\ \boldsymbol{w} = 0, & on\ \Gamma. \end{cases} \tag{10}$$

3. Variational level set formulation

Considering the working domain $\mathcal{D} \subset \mathbb{R}^2$, we assume there exists a implicit function $\phi(x)$, the so-called level set function, which satisfies

$$\begin{cases} \phi(x) > 0, & \forall x \in \Omega \\ \phi(x) = 0, & \forall x \in \Gamma := \partial\Omega \\ \phi(x) < 0. & \forall x \in \mathcal{D} \setminus \overline{\Omega}. \end{cases} \tag{11}$$

The local unit normal $\boldsymbol{n}$ and curvature κ to the surface are given by

$$\boldsymbol{n} = \frac{\nabla \phi}{|\nabla \phi|}, \tag{12}$$

and

$$\kappa = \nabla \cdot \boldsymbol{n} = \operatorname{div}\left(\frac{\nabla \phi}{|\nabla \phi|} \right), \tag{13}$$

respectively. In the level set method, it is convenient to use the Heaviside distribution $H(\phi)$ and the Dirac delta distribution $\delta(\phi)$ [39]

$$H(\phi(x)) = \begin{cases} 1, & \phi \geq 0 \\ 0, & \phi < 0 \end{cases} \tag{14}$$

$$\delta(\phi(x)) = \frac{DH(\phi(x))}{D\phi} = \delta(\phi)|\nabla \phi|. \tag{15}$$

For a function $F(x)$, the area integration and the boundary integration are defined respectively as

$$\int_{\Omega} F(x) H(\phi(x)) \mathrm{d}\Omega \tag{16}$$

and

$$\int_{\Gamma} F(x) H(\phi(x)) \mathrm{d}\Gamma = \int_{\Omega} F(x) \delta(\phi(x)) |\nabla \phi(x)| \mathrm{d}\Omega. \tag{17}$$

During the optimization process, the level set function $\phi(x)$ is used to represent the boundaries, as was originally developed for curve and surface evolution [43]. The change of the level set function $\phi(x)$ is governed by the Hamilton–Jacobi equation

$$\frac{\partial \phi(x,t)}{\partial t} - V|\nabla \phi(x,t)| = 0, \tag{18}$$

where V is the desired normal velocity on the boundary.

As mentioned above, it is crucial to keep the level set function as a distance function during the evolution. It is well known that a signed distance function must satisfy the property $|\nabla\phi(x)| = 1$, and vice versa, if any function $\phi(x)$ satisfies $|\nabla\phi(x)| = 1$, then $\phi(x)$ is a signed distance function up to the addition of a constant [8]. So we will use the following integral to characterize how close a function $\phi(x)$ is to a signed distance function in $\Omega \in \mathbb{R}^2$ [34],

$$\mathfrak{D}(\phi(x)) = \int_{\mathcal{D}} \frac{1}{2}(|\nabla\phi| - 1)^2 \mathrm{d}x. \tag{19}$$

If we assume that the normal derivative of $\phi(x)$ vanishes on the boundary

$$\frac{\partial\phi(x)}{\partial \boldsymbol{n}} = 0, \quad \text{on } \partial\mathcal{D} \tag{20}$$

then the Gateaux derivatives of $\mathfrak{D}(\phi(x))$ with respect to $\phi(x)$ in the ψ direction are

$$\left(\frac{\partial\mathfrak{D}(\phi(x))}{\partial\phi}, \psi\right) = -\int_{\mathcal{D}} (\Delta\phi - \kappa)\psi \mathrm{d}x. \tag{21}$$

In fact,

$$\begin{aligned}
\left(\frac{\partial\mathfrak{D}}{\partial\phi}, \psi\right) &= \lim_{t\to 0} \frac{\int_{\mathcal{D}} \frac{1}{2}(|\nabla(\phi + t\psi)| - 1)^2 \mathrm{d}x - \int_{\mathcal{D}} \frac{1}{2}(|\nabla\phi| - 1)^2 \mathrm{d}x}{t} \\
&= \int_{\mathcal{D}} \frac{1}{2} \lim_{t\to 0} \frac{2t\nabla\phi\cdot\nabla\psi + t^2|\nabla\psi|^2 - 2|\nabla(\phi + t\psi)| - 2|\nabla\phi|}{t} \mathrm{d}x \\
&= \int_{\mathcal{D}} \left(\nabla\phi\cdot\nabla\psi - \lim_{t\to 0} \frac{|\nabla(\phi + t\psi)|^2 - |\nabla\phi|^2}{t(|\nabla(\phi + t\psi)| + |\nabla\phi|)}\right) \mathrm{d}x \\
&= \int_{\mathcal{D}} \left(\nabla\phi\cdot\nabla\psi - \frac{\nabla\phi\cdot\nabla\psi}{|\nabla\phi|}\right) \mathrm{d}x \\
&= -\int_{\mathcal{D}} (\Delta\phi - \kappa)\psi \mathrm{d}x + \int_{\Gamma} \psi \frac{\partial\phi}{\partial \boldsymbol{n}} \mathrm{d}\Gamma + \int_{\Gamma} \frac{\psi}{|\nabla\phi|} \frac{\partial\phi}{\partial \boldsymbol{n}} \mathrm{d}\Gamma \quad \text{(by Eq. (20))} \\
&= -\int_{\mathcal{D}} (\Delta\phi - \kappa)\psi \mathrm{d}x.
\end{aligned}$$

From Theorem 3, the shape derivative can be written as the following form

$$\mathscr{D}\mathcal{J}(\Omega)\boldsymbol{h} = \int_{\Gamma} V\boldsymbol{h}\cdot\boldsymbol{n} \mathrm{d}s, \tag{22}$$

where

$$V = \left(\frac{\partial\boldsymbol{u}}{\partial\boldsymbol{n}}\right)^2 - \frac{\partial\boldsymbol{u}}{\partial\boldsymbol{n}} \frac{\partial\boldsymbol{w}}{\partial\boldsymbol{n}}. \tag{23}$$

We can define the descent direction by

$$\boldsymbol{h} = -V\boldsymbol{n}. \tag{24}$$

The normal component $\boldsymbol{h}\cdot\boldsymbol{n} = -V$ can be used as the advection velocity in the Hamilton–Jacobi equation (18) [5]. In our proposed algorithm, the level set function will be evolved by

$$\frac{\partial\phi(x,t)}{\partial t} - V|\nabla\phi(x,t)| - \lambda(\Delta\phi(x,t) - \kappa) = 0, \tag{25}$$

where λ is a positive parameter which balances the influence of the force term $(\Delta\phi(x,t) - \kappa)$. The second term on the left-hand side of Eq. (25) drives the zero level set toward the object boundaries, while the third term forces the level set function $\phi(x,t)$ to be close to a signed distance function during the optimization process. The re-initialization procedure is not necessary now.

4. Numerical simulation

4.1. Finite element approximation

The Navier–Stokes equations (1) can be written in component-wise form as:

$$-\nu\Delta u_1 + u_1\frac{\partial u_1}{\partial x_1} + u_2\frac{\partial u_1}{\partial x_2} + \frac{\partial p}{\partial x_1} = f_1, \tag{26}$$

$$-\nu\Delta u_2 + u_1\frac{\partial u_2}{\partial x_1} + u_2\frac{\partial u_2}{\partial x_2} + \frac{\partial p}{\partial x_2} = f_2, \tag{27}$$

where u_i $(i = 1, 2)$ are components of the velocity vector $\boldsymbol{u}$ in respectively the x_i $(i = 1, 2)$ direction and $\boldsymbol{f} = (f_1, f_2)$ is the body force. The continuity equation is:

$$\frac{\partial u_1}{\partial x_1} + \frac{\partial u_2}{\partial x_2} = 0. \tag{28}$$

The Dirichlet boundary conditions are:

$$u_i = 0 \quad (i = 1, 2) \quad \boldsymbol{x} \in \Gamma_c, \tag{29}$$

and

$$u_i = g_i(\boldsymbol{x}) \quad (i = 1, 2) \quad \boldsymbol{x} \in \Gamma_d. \tag{30}$$

g_1 and g_2 satisfy the compatibility condition (2).

For system (26)–(28) we can derive the corresponding Galerkin equations:

$$\int_\Omega \left[\nu\nabla u_{h1}\cdot\nabla\phi_i + \left(u_{h1}\frac{\partial u_{h1}}{\partial x_1} + u_{h2}\frac{\partial u_{h1}}{\partial x_2}\right)\phi_i - p\frac{\partial\phi_i}{\partial x_1}\right]\mathrm{d}\Omega = \int_\Omega f_1\phi_i\,\mathrm{d}\Omega, \tag{31}$$

$$\int_\Omega \left[\nu\nabla u_{h2}\cdot\nabla\phi_i + \left(u_{h1}\frac{\partial u_{h2}}{\partial x_1} + u_{h2}\frac{\partial u_{h2}}{\partial x_2}\right)\phi_i - p\frac{\partial\phi_i}{\partial x_1}\right]\mathrm{d}\Omega = \int_\Omega f_2\phi_i\,\mathrm{d}\Omega,$$
$$(i = 1, 2, \ldots, N), \tag{32}$$

$$\int_\Omega \left[\frac{\partial u_1}{\partial x_1} + \frac{\partial u_2}{\partial x_2}\right]\psi_j\,\mathrm{d}\Omega = 0, \quad (j = 1, 2, \ldots, M). \tag{33}$$

The above equations contain, due to the convection, nonlinear terms of the type:

$$u_{h1}\frac{\partial u_{h1}}{\partial x_1} = \sum_{j=1}^{N}\sum_{k=1}^{N} u_{1j}u_{1k}\phi_j\frac{\partial\phi_k}{\partial x_1}, \tag{34}$$

with u_{1j} and u_{1k} as unknowns.

For all our calculations, we apply a Taylor–Hood element $(P_2 - P_1)$ discretization of the Navier–Stokes equations, i.e.

$$u_{hi} = \sum_{j=1}^{6} u_{ij}\phi_j, \tag{35}$$

with

$$a_j(2\lambda_j - 1), \quad j = 1, 2, 3, \tag{36}$$

$$\phi_4 = 4\lambda_2\lambda_3, \qquad \phi_5 = \lambda_1\lambda_3, \qquad \phi_6 = 4\lambda_1\lambda_2, \tag{37}$$

and $p_h = \sum_{j=1}^{3} p_j\psi_j$, with $\psi_j = \lambda_j$, $(j = 1, 2, 3)$. u_{ij} and p_j are the nodal point values of velocity and pressure and λ_j the linear polynomials for a triangular element. This is a stable element in standard fluid mechanics [52]. The shape derivative of the cost functional (9) and the adjoint equations (10) can also be treated in the same way.

4.2. Numerical implementation of the variational level set method

From the point of view of computation, the smeared-out Heaviside and Dirac delta distributions are preferred during the optimization process. We use the following regularized Heaviside and Dirac delta functions in our numerical examples:

$$H_\rho(x) = \begin{cases} 1 & \text{if } x > \rho, \\ 0 & \text{if } x < -\rho, \\ \frac{1}{2}\left[1 + \frac{x}{\rho} + \frac{1}{\pi}\sin\left(\frac{\pi x}{\rho}\right)\right] & \text{if } |x| \le \rho. \end{cases} \tag{38}$$

$$\delta_\rho(x) = \begin{cases} 0 & \text{if } |x| > \rho, \\ \frac{1}{2\rho}\left[1 + \cos\left(\frac{\pi x}{\rho}\right)\right] & \text{if } |x| \le \rho, \end{cases} \tag{39}$$

where ρ is a tunable parameter that determines the size of the bandwidth of numerical smearing. A typically good value is $\rho = 1.5\Delta x$, where Δx is the grid size [40].

Before we move on, we introduce some notations concerning the differences. We define

$$\delta_+^x \phi_{l,m} = \frac{\phi_{l+1,m} - \phi_{l,m}}{\Delta x}, \qquad \delta_+^y \phi_{l,m} = \frac{\phi_{l,m+1} - \phi_{l,m}}{\Delta y};$$

$$\delta_-^x \phi_{l,m} = \frac{\phi_{l,m} - \phi_{l-1,m}}{\Delta x}, \qquad \delta_-^y \phi_{l,m} = \frac{\phi_{l,m} - \phi_{l,m-1}}{\Delta y};$$

$$\delta_0^x \phi_{l,m} = \frac{\phi_{l+1,m} - \phi_{l-1,m}}{2\Delta x}, \qquad \delta_0^y \phi_{l,m} = \frac{\phi_{l,m+1} - \phi_{l,m-1}}{2\Delta y};$$

$$\delta_c^x \phi_{l,m} = \frac{\phi_{l+1,m} - 2\phi_{l,m} + \phi_{l-1,m}}{(\Delta x)^2}, \qquad \delta_c^y \phi_{l,m} = \frac{\phi_{l,m+1} - 2\phi_{l,m} - \phi_{l,m-1}}{(\Delta y)^2}$$

to be forward, backward, centered and centered second difference, respectively.

Practical experience suggests that temporal truncation errors seem to produce less deterioration of the numerical solution in level set methods, so we use the following simple time step algorithm to evolve the level set function ϕ in (25):

$$\frac{\phi^{i+1} - \phi^i}{\Delta t} - V^i \left|\nabla \phi^i\right| - \lambda^i(\Delta\phi^i - \kappa^i) = 0, \tag{40}$$

where Δt is the time step ($i = 0, 1, 2, \ldots$) and ϕ^0 is known a priori. On the other hand, the level set methods are sensitive to spatial accuracy. In order to avoid oscillations, we employ the high order ENO (essentially nonoscillatory) scheme in our calculations [45]:

(i) if $V^i < 0$, then

$$\left|\nabla \phi_{jk}\right| = \sqrt{(\max(D_-^x \phi_{jk}, 0))^2 + (\min(D_+^x \phi_{jk}, 0))^2 + (\max(D_-^y \phi_{jk}, 0))^2 + (\min(D_+^y \phi_{jk}, 0))^2}$$

(ii) if $V^i \ge 0$, then

$$\left|\nabla \phi_{jk}\right| = \sqrt{(\min(D_-^x \phi_{jk}, 0))^2 + (\max(D_+^x \phi_{jk}, 0))^2 + (\min(D_-^y \phi_{jk}, 0))^2 + (\max(D_+^y \phi_{jk}, 0))^2}$$

where j, k are the index for the x and y coordinates and

$$D_-^x \phi_{jk} = \delta_-^x \phi_{j,k} + \frac{\Delta x}{2}\mathcal{M}\left[\delta_c^x \phi_{j,k}, \delta_c^x \phi_{j-1,k}\right],$$

$$D_+^x \phi_{jk} = \delta_+^x \phi_{j,k} + \frac{\Delta x}{2}\mathcal{M}\left[\delta_c^x \phi_{j+1,k}, \delta_c^x \phi_{j,k}\right],$$

$$D_-^y \phi_{jk} = \delta_-^y \phi_{j,k} + \frac{\Delta y}{2}\mathcal{M}\left[\delta_c^y \phi_{j,k}, \delta_c^y \phi_{j,k-1}\right],$$

$$D_+^y \phi_{jk} = \delta_+^y \phi_{j,k} + \frac{\Delta y}{2}\mathcal{M}\left[\delta_c^y \phi_{j,k+1}, \delta_c^y \phi_{j,k}\right],$$

where

$$\mathcal{M}[X, Y] = \begin{cases} \min(X, Y) & \text{if } X \cdot Y > 0, \\ 0 & \text{if } X \cdot Y \leq 0. \end{cases} \tag{41}$$

The curvature term is approximated by using

$$\nabla \cdot \left(\frac{\nabla \phi}{|\nabla \phi|} \right) = \left(\frac{\phi_x}{|\nabla \phi|} \right)_x + \left(\frac{\phi_y}{|\nabla \phi|} \right)_y, \tag{42}$$

so

$$\begin{aligned} \nabla \cdot \left(\frac{\nabla \phi}{|\nabla \phi|} \right)_{jk} = & \left[\left(\frac{\phi_x}{|\nabla \phi|} \right)_{j+1/2,k} - \left(\frac{\phi_x}{|\nabla \phi|} \right)_{j-1/2,k} \right] \Big/ \Delta x \\ & + \left[\left(\frac{\phi_y}{|\nabla \phi|} \right)_{j,k+1/2} - \left(\frac{\phi_y}{|\nabla \phi|} \right)_{j,k-1/2} \right] \Big/ \Delta y, \end{aligned} \tag{43}$$

where

$$\left(\frac{\phi_x}{|\nabla \phi|} \right)_{j+1/2,k} = \frac{\delta_+^x \phi_{j,k}}{\sqrt{(\delta_+^x \phi_{j,k})^2 + \left[\frac{1}{2} \left(\delta_0^y \phi_{j,k} + \delta_0^y \phi_{j+1,k} \right) \right]^2}}$$

$$\left(\frac{\phi_x}{|\nabla \phi|} \right)_{j-1/2,k} = \frac{\delta_-^x \phi_{j,k}}{\sqrt{(\delta_-^x \phi_{j,k})^2 + \left[\frac{1}{2} \left(\delta_0^y \phi_{j-1,k} + \delta_0^y \phi_{j,k} \right) \right]^2}}$$

$$\left(\frac{\phi_y}{|\nabla \phi|} \right)_{j,k+1/2} = \frac{\delta_+^y \phi_{j,k}}{\sqrt{(\delta_+^y \phi_{j,k})^2 + \left[\frac{1}{2} \left(\delta_0^x \phi_{j,k} + \delta_0^x \phi_{j,k+1} \right) \right]^2}}$$

$$\left(\frac{\phi_y}{|\nabla \phi|} \right)_{j,k-1/2} = \frac{\delta_+^y \phi_{j,k}}{\sqrt{(\delta_+^y \phi_{j,k})^2 + \left[\frac{1}{2} \left(\delta_0^x \phi_{j,k-1} + \delta_0^x \phi_{j,k} \right) \right]^2}}.$$

4.3. Optimization algorithm

Based on the above results, we can obtain the following algorithm:

(1) Initialization of the level set function $\phi_0(x)$ corresponding to an initial domain Ω_0.
(2) Iteration until convergence, for $i \geq 0$:
- Compute the state $\boldsymbol{u}_i$ and adjoint state $\boldsymbol{w}_i$ through two problems (1) and (10), then obtain the shape derivative of the cost functional by (9).
- Deform the shape by solving the modified Hamilton–Jacobi equation (25). The new shape Ω_{i+1} is characterized by the zero-contour of the level set function ϕ_{i+1}.

It can be seen that the re-initialization procedure can be ignored now.

4.4. Numerical examples

We will present two benchmark numerical examples for two-dimensional shape optimization in this section, which can be commonly found in the fluid mechanics literature and have been used by several authors recently [11,17,25], to verify the promising features of our proposed algorithm.

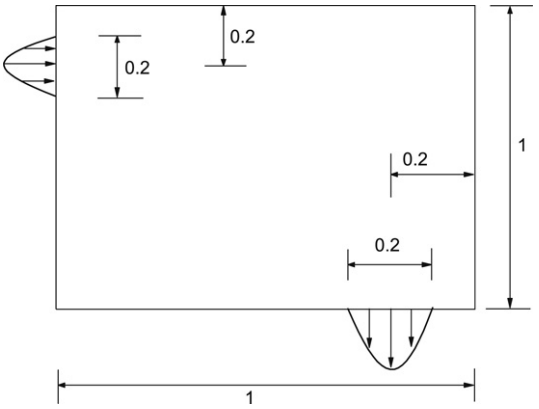

Fig. 1. Design domain for the pipe bend example [11].

In both the experimental results shown in this section the parameter λ is equal to 1. The time step Δt can be chosen much larger than that of the conventional level set method. But in order to ensure the stability of the evolution, we use $\Delta t \leq 5$ in all our examples. The design domains are discretized into 150×150 elements. The present algorithm terminated when the relative difference between two successive cost functional values is less than the prescribed error.

4.4.1. Design of a bend

In the first numerical example, we consider the design of a bend, which can be found in [11] and [17]. The design domain is shown in Fig. 1. The initial shape is the full domain. Our target is to find the efficient connection between the inlet and outlet subject to the constraint that the fluid is allowed to occupy a quarter of the domain. We consider two situations, Navier–Stokes flow with the Reynolds numbers $Re = 10$ and $Re = 1000$. The initial and the final velocity field with streamlines are shown in Fig. 2. The convergence history of the objective functional (3) is shown in Fig. 3.

It can be seen from Fig. 2(b) that our method successfully obtains the pipe bend which is similar to that of [11] and [17]. From the final design in Fig. 2, we also see that the pipe has a sharp bend for low Reynolds number as in the Stokes problem. As the Reynolds numbers increased the corners become rounder.

4.4.2. A diffuser

In the second numerical example, we demonstrate our algorithm by a diffuser. This problem was previous studied in [11] and [25].

The design domain is shown in Fig. 4 and also treated as dimensionless as in [25]. The maximum inlet velocity is 1 and the maximum outlet velocity is 3. The velocity is prescribed to be zero elsewhere on the boundary of the domain. The prescribed volume fraction is $\gamma = 0.5$. The initial shape is also the full domain as depicted in Fig. 5. The Reynolds numbers is 1000. The optimal shape is shown in Fig. 6 which is similar to those in [11] and [25]. Fig. 7 shows the evolution of the objective functional. As can be seen, the convergence speed is also satisfactory.

5. Conclusions

We have proposed a method for shape or topology optimization of the Navier–Stokes problem in the present paper. This method has the following advantages over the existing methods:

- The level set method in our formulation can be easily implemented and is computationally more efficient since it is an Eulerian shape capture method and a re-initialization procedure is not necessary;
- It is insensitive to the initial shape or topology, such that the level set function can be initialized with any distance functions with any shape or topology that are more efficient to construct and easier to use in practice;
- It allows for drastic topology changes during the optimization process.

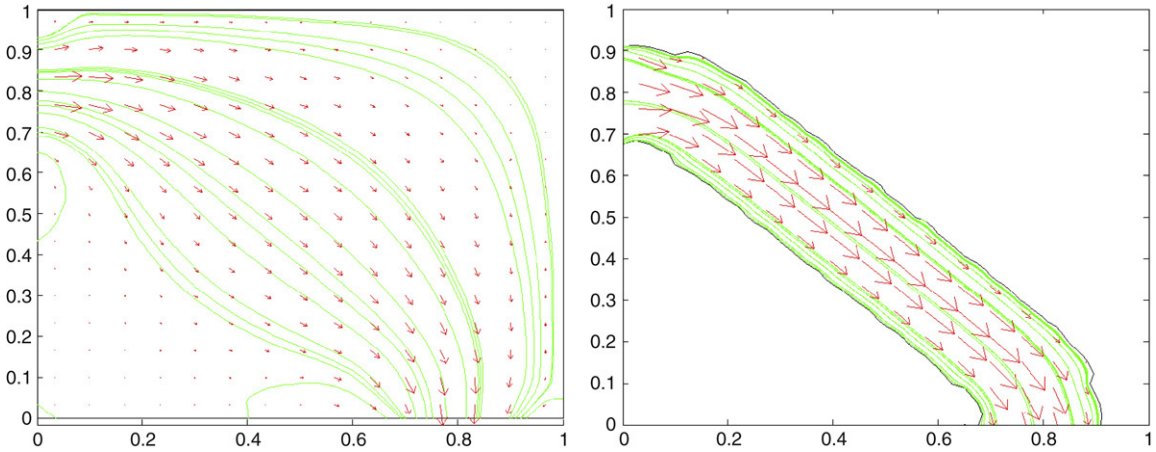

(a) The initial and the final velocity field with streamlines ($Re = 10$).

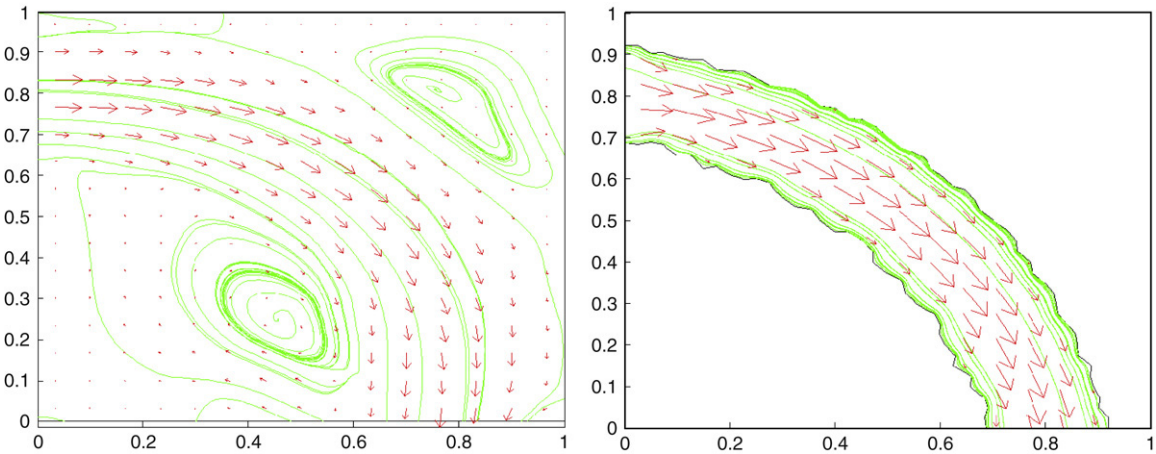

(b) The initial and the final velocity field with streamlines ($Re = 1000$).

Fig. 2. The initial and the final velocity field with streamlines for different Reynolds numbers.

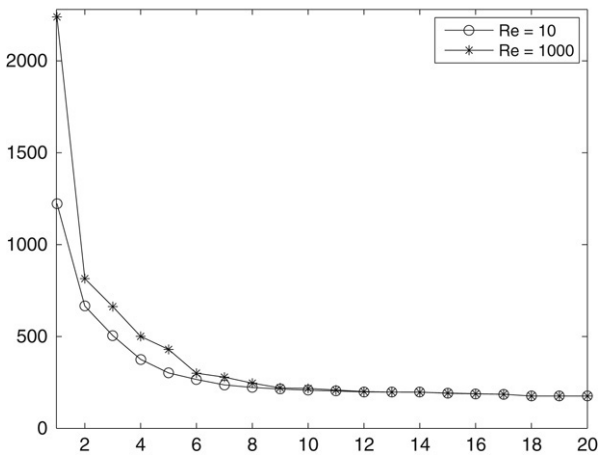

Fig. 3. Convergence history of the objective functional.

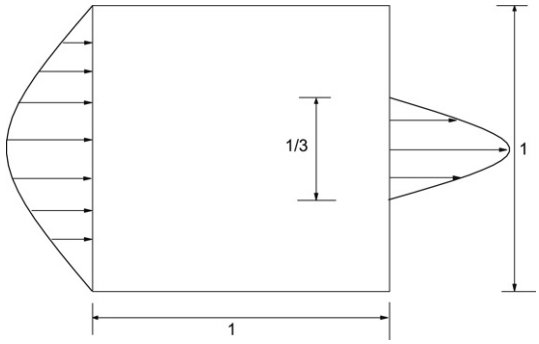

Fig. 4. The design domain for the diffuse example [11].

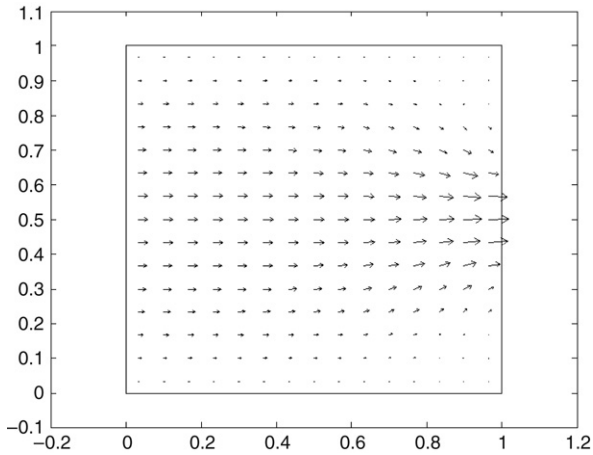

Fig. 5. The initial velocity field.

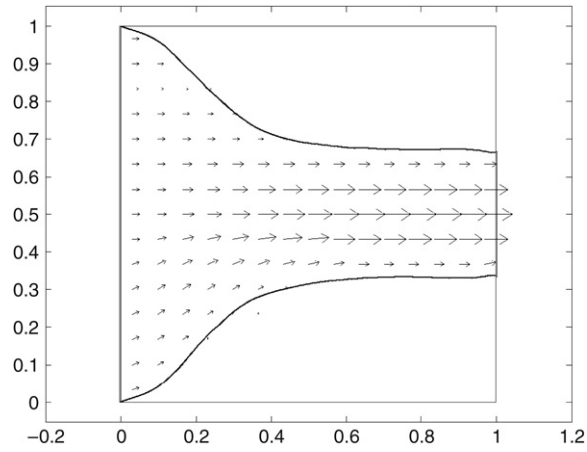

Fig. 6. Optimal diffuser.

The provided numerical examples illustrate that the present algorithm is successful in accuracy, convergence speed and insensitivity to initial shape or topology.

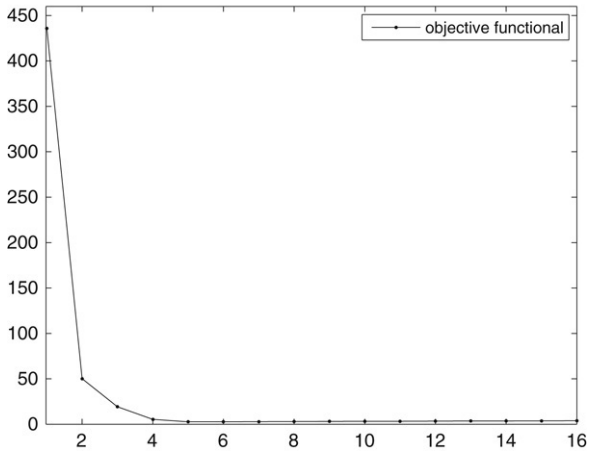

Fig. 7. Convergence history of the objective functional.

Acknowledgements

The authors would like to thank the editor and referees for their valuable comments and suggestions that helped us to improve this paper.

References

[1] L. Adams, Z.L. Li, The immersed interface/multigrid methods for interface problems, SIAM J. Sci. Comput. 24 (2) (2002) 463–479.
[2] V. Agoshkov, A. Quarteroni, G. Rozza, A mathematical approach in the design of arterial bypass using unsteady Stokes equations, J. Sci. Comput. 28 (2–3) (2006) 139–161.
[3] V. Agoshkov, A. Quarteroni, G. Rozza, Shape design in aorto-coronaric bypass anastomoses using perturbation theory, SIAM J. Numer. Anal. 44 (1) (2006) 367–384.
[4] G. Allaire, F. Jouve, A.M. Toader, A level-set method for shape optimization, C. R. Acad. Sci. Paris, Ser. I, 334, 1125–1130.
[5] G. Allair, F. Jouve, A.M. Toader, Structural optimization using sensitivity analysis and a level-set method, J. Comput. Phys. 194 (2004) 363–393.
[6] J.J. Alonso, I.M. Kroo, A. Jameson, Advanced algorithms for design and optimization of QSP, AIAA, 2002–0144.
[7] S. Amstutz, H. Andrä, A new algorithm for topology optimization using a level-set method, J. Comput. Phys. 216 (2) (2006) 573–588.
[8] V.I. Arnold, Geometrical Methods in the Theory of Ordinary Differential equations, Springer-Verlag, New York, 1983.
[9] F. Bauer, P. Garabedian, D. Korn, A. Jameson, Supercritical Wing Sections, Springer, Berlin, 1972.
[10] M. Bendsoe, O. Sigmund, Topology optimization, Theory, Methods and Applications, Springer Verlag, New York, 2003.
[11] T. Borrvall, J. Petersson, Topology optimization of fluid in Stokes flow, Int. J. Numer. Meth. Fl. 41 (2003) 77–107.
[12] T. Chan, L. Vese, Active contours without edges, IEEE T. Image. Process 10 (2001) 266–277.
[13] J.A. Desideri, B.A. El Majd, A. Janka, Nested and self-adaptive Bezier parameterizations for shape optimization, J. Comput. Phys. 224 (1) (2007) 117–131.
[14] J.A. Desideri, J.P. Zolesio, Inverse shape optimization problems and application to airfoils, Control. Cybern. 34 (1) (2005) 165–202.
[15] Q. Du, M. Gunzburger, J. Lee, Optimization-based methods for multidisciplinary simulation and optimization, in: Proc. 8th Annual Conference of the CFD Society of Canada, CERCA, Montreal, 2000, pp. 689–694.
[16] Z.M. Gao, Y.C. Ma, Shape sensitivity analysis for a Robin problem via minimax differentiability, Appl. Math. Comput. 181 (2) (2006) 1090–1105.
[17] A. Gersborg-Hansen, O. Sigmund, R.B. Haber, Topology optimization of channel flow problems, Struct. Multidiscip. O. 30 (2005) 181–192.
[18] V. Girault, P. Raviart, Finite Element Methods for Navier–Stokes Equations: Theory and Algorithms, Springer-Verlag, Berlin, Heidelberg, 1986.
[19] R. Glowinski, Y. Kuznetsov, Distributed Lagrange multipliers based on fictitious domain method for second order elliptic problems, Comput. Method Appl. M. 196 (8) (2007) 1498–1506.
[20] R. Glowinski, T.W. Pan, T.I. Hesla, D.D. Joseph, A distributed lagrange multiplier/fictitious domain method for particulate flows, Int. J. Mutiphase Flow 25 (5) (1999) 755–794.
[21] R. Glowinski, T.W. Pan, T.I. Hesla, D.D. Joseph, J. Periaux, A distributed Lagrange multiplier/fictitious domain method for the simulation of flows around moving rigid bodies: Application to particulate flow, Comput. Method Appl. M. 184 (2–4) (2000) 241–267.
[22] R. Glowinski, T.W. Pan, T.I. Hesla, D.D. Joseph, J. Periaux, A fictitious domain approach to the direct numerical simulation of incompressible viscous flow past moving rigid bodies: Application to particulate flow, J. Comput. Phys. 169 (2) (2001) 363–426.

[23] R. Glowinski, T.W. Pan, J. Periaux, Numerical simulation of a multi-store separation phenomenon: A fictitious domain approach, Comput. Method Appl. M. 195 (41–43) (2006) 5566–5581.
[24] R. Glowinski, T.W. Pan, J. Periaux, A fictitious domain method for Dirichlet problem and applications, Comput. Method Appl. M. 111 (3) (1994) 283–303.
[25] J.K. Guest, J.H. Prevost, Topology optimization of creeping fluid flows using a Darcy–Stokes finite element, Int. J. Numer. Meth. Eng. 66 (2006) 461–484.
[26] M. Gunzburger, H. Kim, Existence of an optimal solution of a shape control problem for the stationary Navier–Stokes equations, SIAM J. Control. Optim. 36 (3) (1998) 895–909.
[27] M. Gunzburger, C. Trenchea, Analysis of an optimal control problem for the three-dimensional coupled modified Navier–Stokes and Maxwell equations, J. Math. Anal. Appl. 333 (1) (2007) 295–310.
[28] M.D. Gunzburger, Perspectives in Flow Control and Optimization, SIAM, Philadelphia, 2003.
[29] J. Haslinger, Comparison of different fictitious domain approaches used in shape optimization, Technical Report 15, University of Jyväskylä, Department of Mathematics, 1996.
[30] J. Haslinger, T. Kozubek, K. Kunisch, G. Peichl, Shape optimization and fictitious domain approach for solving free boundary problems of Bernoulli type, Comput. Optim. Appl. 26 (2003) 231–251.
[31] A. Jameson, Aerodynamic design and optimization, in: 16th AIAA Comput. Fluid Dynamics Conf., AIAA Pap. A-2003-3438, Orlando, FL, June, 2003, pp. 23–26.
[32] M. Kass, A. Witkin, D. Terzopoulos, Snakes: Active contour models, Int. J. Comput. Vision 1 (1988) 321–331.
[33] R.J. Leveque, Z.L. Li, Immersed interface methods for Stokes flow with elastic boundaries or surface tension, SIAM J. Sci. Comput. 18 (3) (1997) 709–735.
[34] C.M. Li, C.Y. Xu, C.F. Gui, M.D. Fox, Level set evolution without re-initialization: A new variational formulation, CVPR' 05.
[35] Z.L. Li, Immersed interface methods for moving interface problems, Numer. algorithms 14 (4) (1997) 269–293.
[36] B. Mohammadi, O. Pironneau, Applied Shape Optimization for Fluids, Clarendon Press, Oxford, 2001.
[37] B. Mohammadi, O. Pironneau, Shape optimization in fluid mechanics, Annu. Rev. Fluid Mech. 36 (2004) 255–279.
[38] S. Osher, F. Santosa, Level-set methods for optimization problems involving geometry and constraints: Frequencies of a two-density inhomogeneous drum, J. Comput. Phys. 171 (2001) 272–288.
[39] S. Osher, J.A. Sethian, Fronts propagating with curvature-dependent speed: Algorithms based on Hamilton–Jacobi formulations, J. Comput. Phys. 79 (1988) 12–49.
[40] S. Osher, J.A. Sethian, Level Set Methods and Dynamic Implicit Surface, Springer-Verlag, 2002.
[41] A. Quarteroni, G. Rozza, Optimal control and shape optimization of aorto-coronaric bypass anastomoses, Math. Mod. Meth. Appl. S. 13 (12) (2003) 1801–1823.
[42] J. Reuther, A. Jameson, J. Farmer, L. Martinelli, D. Saunders, Aerodynamic shape optimization of complex aircraft configurations via an adjoint formulation, AIAA 96 (1996) 94.
[43] J.A. Sethian, Level Set Methods and Fast Marching Methods: Evolving Interfaces in Computational Geometry, Fluid Mechanics, Computer Vision and Materials Science, Cambridge University Press, 1999.
[44] J.A. Sethian, A. Wiegmann, Structural boundary design via level set and immersed interface methods, J. Comput. Phys. 163 (2) (2000) 489–528.
[45] C.W. Shu, S. Osher, Efficient implementation of essentially non-oscillatory shock-capturing schemes, J. Comput. Phys. 77 (2) (1988) 439–471.
[46] J. Sokolowski, J.P. Zolesio, Introduction to Shape Optimization: Shape Sensitivity Analysis, in: Springer Series in Computational Mathematics, Springer, Berlin, 1992.
[47] R. Temam, Navier–Stokes Equations: Theory and Numerical Analysis, AMS Chelsea Publishing, 2000.
[48] M.Y. Wang, X. Wang, PDE-driven level sets, shape sensitivity and curvature flow for structural topology optimization, CMES-Comp. Model. Eng. 6 (4) (2004) 373–395.
[49] M.Y. Wang, X.M. Wang, D.M. Guo, A level set method for structural topology optimization, Comput. Method Appl. M. 192 (2003) 227–246.
[50] W.J. Yan, Y.C. Ma, The application of domain derivative for heat conduction with mixed condition in shape reconstruction, Appl. Math. Comput. 181 (2) (2006) 894–902.
[51] H.K. Zhao, T. Chan, B. Merriman, S. Osher, A variational level set approach to multiphase motion, J. Comput. Phys. 127 (1996) 179–195.
[52] O.C. Zienkiewicz, R.L. Taylor, The Finite Element Method: Fluid Dynamics, 5th edition, vol. 1, Butterworth-Heinemann, Oxford, 2000.